Nickel silicide formation using multiple-pulsed laser annealing

Y. Setiawan[a] and P. S. Lee[b]
School of Materials Science and Engineering, Nanyang Technological University, 50 Nanyang Avenue, Singapore 639798, Singapore

K. L. Pey
Microelectronics Center, School of Electrical and Electronic Engineering, Nanyang Technological University, 50 Nanyang Avenue, Singapore 639798, Singapore

X. C. Wang and G. C. Lim
Singapore Institute of Manufacturing Technology (SIMTech), 71 Nanyang Drive, Singapore 638075, Singapore

F. L. Chow
Chartered Semiconductor Manufacturing Ltd., 60 Woodlands Industrial Park D, Street 2, Singapore 738406, Singapore

(Received 10 July 2006; accepted 29 November 2006; published online 8 February 2007)

The effect of multiple-pulsed laser irradiation on Ni silicide formation in Ni(Ti)/Si system was studied. A layered structure consisting of both crystalline $NiSi_2$ and Ni-rich Ni–Si amorphous phases with a protective TiO_x overlayer was formed after five-pulsed laser annealing at 0.4 J cm^{-2}. Different solidification velocities caused by a variation in the atomic concentration across the melt have led to the formation of this layered structure. On the other hand, by increasing the number of laser pulses, a continuous layer of polycrystalline NiSi was obtained after a 20-pulsed laser annealing at 0.3 J cm^{-2} laser fluence. Its formation is attributed to a better elemental mixing which occurred during subsequent pulses. Enhancement of surface absorption and remelting of the phases formed is proposed as the mechanism governing the continuous NiSi layer formation. © *2007 American Institute of Physics*. [DOI: 10.1063/1.2433707]

I. INTRODUCTION

In complimentary metal-oxide-semiconductor (CMOS) devices, self-aligned silicide (SALICIDE) is formed at the source and drain regions to reduce the contact resistance. Nowadays, Ni silicide (NiSi) is gradually replacing $CoSi_2$ as a silicide material due to its low temperature of formation[1] and less Si consumption.[2] However, formation of Ni silicide has been found to be very sensitive to the presence of native oxide at the Ni/Si interface.[3] Ti capping,[4] Ti interlayer,[5] or Ti alloying[6] has been reported to successfully tackle the problem of residual interfacial oxide. After metal deposition, silicide formation is usually carried out by subjecting the whole device wafer to an elevated temperature for a short duration using rapid thermal annealing (RTA) process. Although this works well with the current metal-oxide-semiconductor field-effect transistor (MOSFET) devices, it might pose some limitations in nanoscale MOSFET devices which incorporate ultrashallow junctions and/or high-*k* dielectrics. Subjecting the whole wafer to a high thermal budget process might induce undesired dopant diffusion and/or crystallization of high-*k* dielectric.

Tung *et al.* reported the possibility of using laser irradiation to form high quality epitaxial silicides such as $CoSi_2$ and $NiSi_2$ on Si(111) through liquid phase epitaxial regrowth.[7] However, due to the complexity of the laser annealing process and unavailability of reliable laser source back in the late 1980s, the laser annealing was left dormant for decades, and the RTA process was adopted as the standard method to form silicide in microelectronic industry. Nonetheless, recently there is a growing trend in exploring laser in both junction activation applications[8,9] as well as in the silicide formation.[10,11] This is due to the versatility and ability of laser to locally anneal the device wafer. Laser annealing can provide ultrafast annealing with a very limited thermal energy that is just enough to form silicide and minimize the change in the overall diffusion profile of the junction. In addition, recent study which utilized laser annealing to reduce the Ge out segregation in $Ni/Si_{0.76}Ge_{0.24}$ and $Ni/Si_{1-x-y}Ge_xC_y$ systems has resulted in Ni digermanosilicide formation.[12,13] All literature mentioned above reported the formation of Si-rich phases [e.g., Ni digermanosilicide, $NiSi_2$, and $CoSi_2$ (Ref. 14)] which are common and easily achieved using laser annealing. This phenomenon is caused by the nature of the laser beam itself which irradiates a high energy pulse on the sample surface. In the case of $CoSi_2$, the formation of Si-rich compound is desired, since it exhibits the lowest resistivity. However, in the case of Ni silicidation, instead of $NiSi_2$, NiSi phase has the lowest resistivity.[1] This requirement might bring a great challenge in utilizing a high energy laser annealing to induce NiSi formation. Attempt on forming a metastable epitaxial NiSi using a preformed NiSi/Si system before laser annealing has been reported.[15] As such, efforts on demonstrating direct Ni monosilicide formation in $Ni_{1-x}(Ti)_x/Si$ sample using multiple-pulsed laser

[a]Electronic mail: yudi0001@ntu.edu.sg
[b]Electronic mail: pslee@ntu.edu.sg

0021-8979/2007/101(3)/034307/5/$23.00 © 2007 American Institute of Physics

Downloaded 30 Jun 2011 to 155.69.4.4. Redistribution subject to AIP license or copyright; see http://jap.aip.org/about/rights_and_permissions

annealing is pursued in this work. Ti was added into the Ni film to reduce oxidation problem that might arise during high energy laser annealing.

II. EXPERIMENTAL SETUP

A thin layer of Ni–Ti alloy was deposited on *p*-Si(100) substrate. Prior to the metal deposition, the wafer was cleaned using standard Radio Corporation of America (RCA) solution followed by diluted hydrofluoric acid (HF) solution (1:50) dip to remove the native oxide. The wafer was immediately loaded into a sputtering chamber to minimize contamination. A short presputtering was performed before deposition of a 100 nm thick metal layer from a Ni–Ti alloy target (23.5 at. % of Ti) with a deposition rate of about 3.3 Å/s. Excimer laser irradiation (λ:248 nm; full width at half maximum (FWHM): 23 ns) was then carried out on the as-deposited samples using a Lambda Physik laser generator under continuous purified N_2 purging. Multiple-pulsed (5- and 20-pulsed) laser annealing using laser fluences ranging from 0.2 to 0.5 J cm^{-2} was used to study the effect of repeated laser irradiation on Ni silicidation. The laser spot size was about 6×2 mm^2. X-ray diffraction (XRD) analysis was employed to determine the phases formed. Cross-sectional transmission electron microscopy (XTEM) analyses were done using a JEM2010 TEM system. Four-point probe measurements were performed on the laser annealed samples to monitor their sheet resistance evolution. The diffuse surface reflectance of the sample at 248 nm laser irradiation was measured using UV-visible measurement to observe laser induced surface modification of the sample.

III. RESULTS AND DISCUSSION

The as-deposited film exhibited columnar polycrystalline grains with an intermixing of Ni–Ti–Si atoms in a form of amorphous layer within the first few nanometers of the $Ni_{1-x}(Ti)_x$/Si interface. The formation of this amorphous interlayer was caused by a weakening of Si bond upon adsorption of $Ni_{1-x}(Ti)_x$ atoms on Si surface during the sputter deposition process. The selected area electron diffraction (SAED) of the as-deposited $Ni_{1-x}(Ti)_x$ film (not shown) exhibited a typical cubic ring pattern suggesting that no intermetallic Ni–Ti compound (i.e., Ni_3Ti) was formed. The absence of diffraction lines other than the one from $Ni_{1-x}(Ti)_x$ film in the SAED pattern also indicates that Ti atoms occupied the substitutional lattice sites in the Ni crystal instead of forming isolated Ti grains which have an hexagonal crystal structure.[16]

As it is observed that the phases formed in the $Ni_{1-x}(Ti)_x$/Si sample were affected by the number of laser pulses, the results of the samples annealed using 5 and 20 laser pulses at varying laser fluences will be described separately.

A. Five-pulsed laser annealing at various laser fluences

The XRD spectra of the samples after five-pulsed laser annealing at various fluences are depicted in Fig. 1. It is apparent that the five-pulsed laser annealing using 0.2 J cm^{-2} laser fluence was insufficient to induce silicidation in the film. Nevertheless, Ti out segregation from Ni lattice to the grain boundaries has occurred. This phenomenon can be observed by a shifting of the $Ni_{1-x}(Ti)_x$ (111) peak to a larger diffraction angle towards the pure Ni (111) peak.[17] Since the position of this shifted peak is located in between the $Ni_{1-x}(Ti)_x$ (111) and Ni (111) peak, it is labeled as $Ni_{1-y}(Ti)_y$ (111) peak, where $y < x$. The absence of the XRD peak originating from compounds other than $Ni_{1-y}(Ti)_y$ indicates that the five-pulsed laser annealing at 0.3 J cm^{-2} might have only enhanced an intermixing of Ni, Ti, and Si atoms at $Ni_{1-y}(Ti)_y$/Si interface. This intermixing resulted in the formation of a thicker amorphous interlayer with no and/or minimal silicide formation, thus yielding a reduction of the $Ni_{1-y}(Ti)_y$ (111) peak intensity. The reaction started to occur after five-pulsed laser annealing at 0.4 J cm^{-2} where $NiSi_2$ and small amount of NiSi were detected in the XRD spectra. Eventually, $NiSi_2$ became the predominant phase after annealing at higher laser fluences such as 0.5 J cm^{-2}.

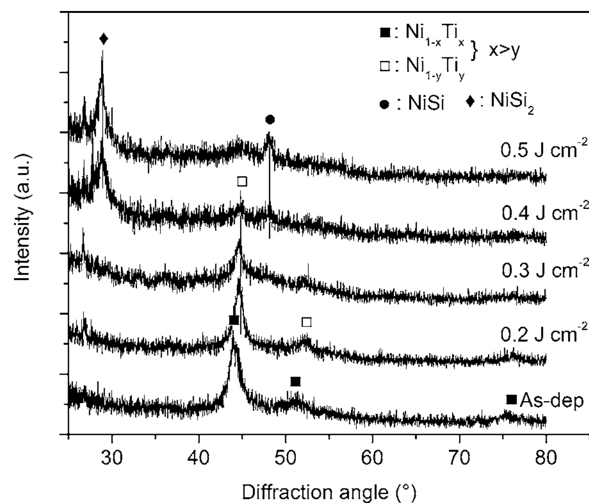

FIG. 1. XRD spectra of $Ni_{1-x}(Ti)_x$/Si sample after five-pulsed laser annealing for both as-deposited and annealed samples.

The effect of five-pulsed laser irradiation on the microstructure and crystallinity of the resulting silicide was studied using XTEM. The XTEM analysis of the sample subjected to a five-pulsed laser annealing at 0.4 J cm^{-2} is shown in Fig. 2. As observed in Fig. 2, the sample annealed using the five-pulsed laser annealing at 0.4 J cm^{-2} exhibits a complex three-layered structure with a presence of crystalline $NiSi_2$ at the film/Si interface followed by a Ni-rich Ni–Si amorphous layer and TiO_x layer at the surface. The formation of layered structure in the sample after the five-pulsed laser annealing at 0.4 J cm^{-2} can be explained as follows. It is believed that during five-pulsed laser annealing at 0.4 J cm^{-2}, the laser energy absorbed by the sample was able to melt the whole $Ni_{1-y}(Ti)_y$ layer together with a few hundreds of angstroms of Si substrate. The melting and resolidification processes occurred so rapidly that it did not allow the atoms to redistribute inside the melt. This created a film with varying Ni–Si concentration starting with a Si-rich region at the film/Si interface and gradually became a Ni-rich region at the surface. From the Ni–Si phase diagram, the Ni-rich compound such as Ni_2Si has a considerably higher

Downloaded 30 Jun 2011 to 155.69.4.4. Redistribution subject to AIP license or copyright; see http://jap.aip.org/about/rights_and_permissions

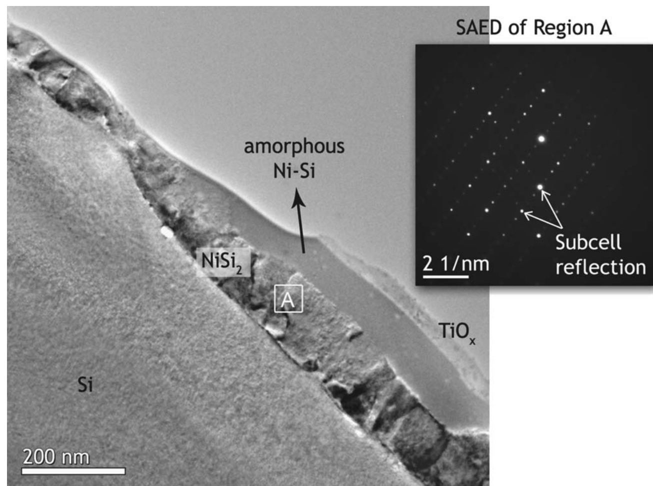

FIG. 2. XTEM bright field micrograph of $Ni_{1-x}(Ti)_x/Si$ sample after five-pulsed laser annealing at 0.4 J cm^{-2} with the inset showing the SAED pattern of the crystalline $NiSi_2$ layer.

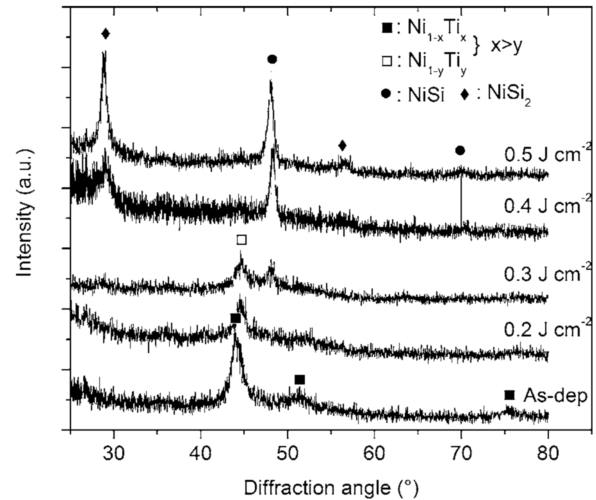

FIG. 3. XRD spectra of $Ni_{1-x}(Ti)_x/Si$ sample after 20-pulsed laser annealing for both as-deposited and annealed samples.

melting temperature (T_m) as compared to Si-rich compound such as $NiSi_2$ (~1310 °C vs ~993 °C).[18] These two layers which have different T_m were in contact with one another. During the solidification process, most of the thermal energy in the molten film was liberated or transferred to the substrate as it has a larger volume (as compared to the thin molten layer at the surface) and would act as a heat sink in the system. Having a higher T_m, the Ni-rich outer layer was severely undercooled and quenched, leaving it as an amorphous layer. On the other hand, the Si-rich inner layer which has lower T_m solidified with a significantly slower speed than the Ni-rich outer layer, allowing the Ni and Si atoms to rearrange themselves in a $NiSi_2$ crystal through liquid phase epitaxial regrowth taking the Si substrate as its template.[10] Ti which has a high affinity towards oxygen was found to out segregate during solidification process, forming a protective TiO_x layer at the surface of the film.

Electron diffraction study of the $NiSi_2$ grain using SAED (inset of Fig. 2) reveals an intercrossing diffraction pattern as well as an appearance of extra diffraction spots (supercell diffraction) in between the $NiSi_2$ subcell diffraction patterns. The former phenomenon is due to twinning of the $NiSi_2$ grains, whereas the latter is caused by a supercell formation, which is basically a tripling of the $NiSi_2$ lattice. Since twinning and supercell formation do not usually occur in a RTA sample,[19–21] their formation is believed to be due to rapid solidification of the $NiSi_2$ layer. It is of interest to note that the $NiSi_2$ phase formed at the interface was uniform without a formation of cellular structures which are occasionally found in laser annealed samples.[14,22] This cellular structure formation is a typical consequence of constitutional supercooling (CSC) phenomenon which is partially caused by a presence of compositional gradient of solute atoms as a function of depth of the molten layer. However, in this experiment, the multiple-pulsed laser annealing has induced a better elemental mixing in the molten film, which reduced the localized compositional gradient and resulted in an absence of CSC.

B. 20-pulsed laser annealing at various laser fluences

Different from the five-pulsed laser annealing, increasing the number of the laser pulses to 20 pulses with laser fluence as low as 0.2 J cm^{-2} was able to cause a significant reduction in the $Ni_{1-y}(Ti)_y$ (111) XRD peak intensity as shown in Fig. 3. Increasing the laser fluence to 0.3 J cm^{-2} has successfully formed a polycrystalline NiSi phase without detectable $NiSi_2$ phase in the sample. Utilizing Scherrer's formula, one can approximate the average grain size of the NiSi phase formed after 20-pulsed laser annealing at 0.3 J cm^{-2} to be about 12.2 nm. This fine grain formation can be attributed to the fact that the NiSi was formed through rapid solidification of the melt during laser annealing. After a 20-pulsed laser annealing at 0.4 J cm^{-2}, a significant growth of NiSi phase, together with an appearance of a new XRD peak originating from $NiSi_2$ (111), was observed. As compared to the 20-pulsed laser annealing at 0.3 J cm^{-2}, the average NiSi grain size after the 20-pulsed laser annealing at 0.4 J cm^{-2} increased by 25% to about 15.7 nm. This is a result of a slower solidification experienced by a hotter molten film induced at higher laser fluence. Finally, $NiSi_2$ and NiSi phases were found to coexist in the sample after a 20-pulsed laser annealing at 0.5 J cm^{-2}.

Similar to the five-pulsed laser annealing at 0.3 J cm^{-2}, a significant reduction in the $Ni_{1-x}(Ti)_x$ (111) peak intensity after a 20-pulsed laser annealing at 0.2 J cm^{-2} was caused by an element intermixing which created an amorphous layer and/or very small amount of silicide at the interface region. It is worth to note that by increasing the number of laser pulses (from 5 to 20 pulses), a similar intermixing could occur at lower laser fluences. This observation indicates that the reaction proceeds in a solid-state manner in low fluence regime [below the melting point (T_m) of the sample] where the diffusion of the elements is affected by the annealing time (i.e., number of laser pulses) and/or the temperature of the sample (i.e., laser fluence). In addition, multiple-pulsed laser annealing was found to enhance the mixing of the elements. This enhancement can be observed by comparing the XRD spectra of the sample after 5-pulsed and 20-pulsed laser anneal-

Downloaded 30 Jun 2011 to 155.69.4.4. Redistribution subject to AIP license or copyright; see http://jap.aip.org/about/rights_and_permissions

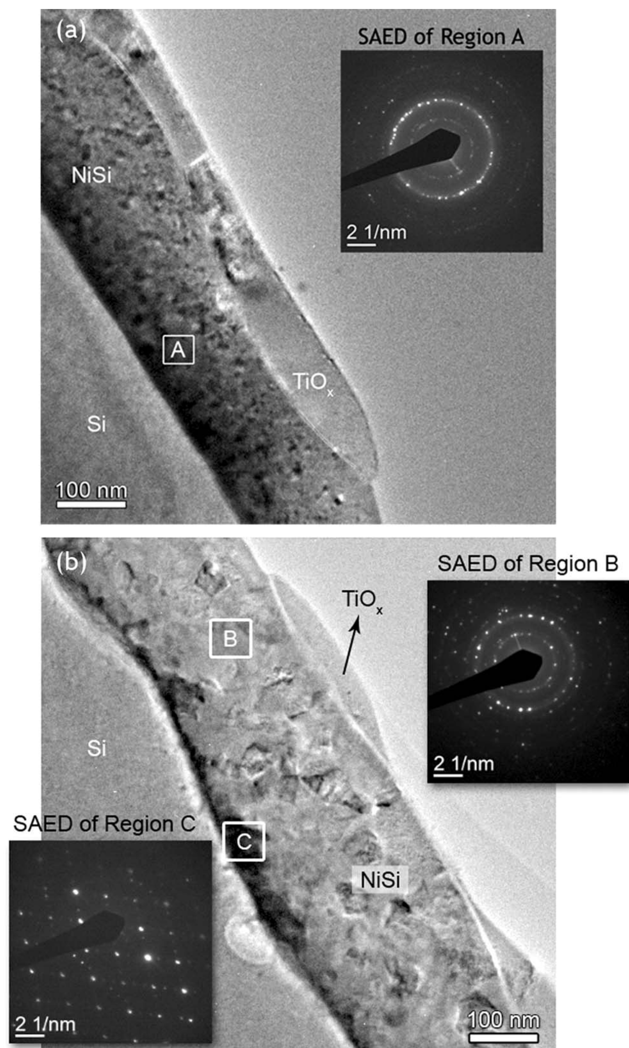

FIG. 4. Bright field XTEM micrographs of $Ni_{1-x}(Ti)_x$/Si sample after 20-pulsed laser annealing at (a) 0.3 J cm^{-2} and (b) 0.5 J cm^{-2}. The insets show the SAED pattern obtained from various conditions shown in (a) and (b).

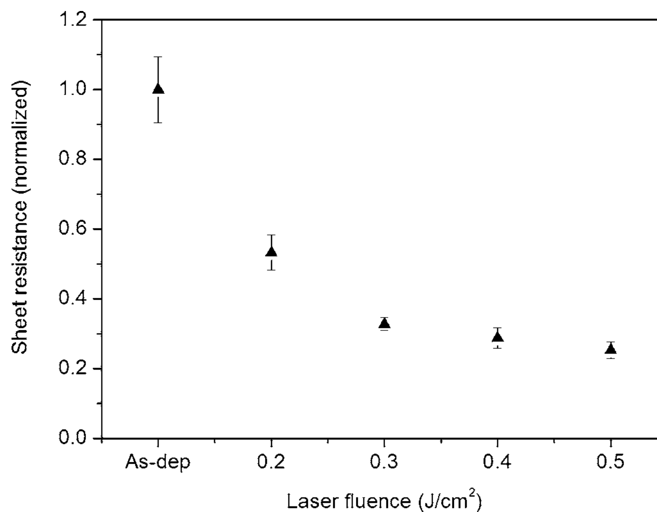

FIG. 5. Sheet resistance (R_s) value of the sample after 20-pulsed laser annealing at different laser fluences (0.2–0.5 J cm^{-2}). The sheet resistances of the samples are normalized to that of the as-deposited (as-dep) sample.

ings shown in Figs. 1 and 3, respectively. In the case of five-pulsed laser annealing, with increasing laser fluence, $NiSi_2$ was the first phase found at the silicide/Si interface together with the presence of Ni-rich Ni–Si amorphous overlayer. On the contrary, NiSi was the first phase detected in the sample after 20-pulsed laser annealing. It is believed that increasing the number of laser pulses has induced a better elemental redistribution inside the melt. The NiSi phase formation in the 20-pulsed laser annealed sample was stable until the melt front consumed more Si (for example, due to an increase in the laser fluence >0.4 J cm^{-2}) and hence making $NiSi_2$ formation more favorable at high laser fluence.

The supporting evidence of the above hypothesis can be clearly observed from the XTEM micrograph depicted in Fig. 4(a) where the 20-pulsed laser annealing at 0.3 J cm^{-2} laser fluence was able to enhance the mixing of elements in the film. This enhancement eliminated the formation of multiple-layered structure and the whole film was crystallized into a polycrystalline NiSi. SAED observation on region B of the sample after a 20-pulsed laser annealing at 0.5 J cm^{-2} exhibits a more distinct diffraction spots along the diffraction rings as depicted in the inset of Fig. 4(b). This indicates that bigger grains are present in the sample[23] which agrees well with the XRD analysis in Fig. 3 in which a smaller FWHM of NiSi peak is observed after 20-pulsed laser annealing at 0.5 J cm^{-2} as compared to 0.3 J cm^{-2}. Besides NiSi grain growth which is favorable for resistivity reduction, the 20-pulsed laser annealing at 0.5 J cm^{-2} has caused a nucleation of $NiSi_2$ grains at the film/Si interface. The sheet resistance (R_s) measurement of the sample after the 20-pulsed laser annealing at different laser fluences is normalized to the as-deposited one and plotted in Fig. 5. A high R_s of the as-deposited $Ni_{1-x}(Ti)_x$ film (~25 times higher as compared to pure Ni film on Si substrate) is attributed to an electron scattering caused by Ti atoms which occupied substitutional lattice sites in the $Ni_{1-x}(Ti)_x$ film.[19] Ti outdiffusion to the $Ni_{1-y}(Ti)_y$ grain boundaries minimized the electron scattering caused by Ti atoms which led to a significant reduction of the R_s value of the sample after the 20-pulsed laser annealing at 0.2 J cm^{-2}. Another abrupt drop (~38% reduction) in the R_s value occurred in the sample after the 20-pulsed laser annealing at 0.3 J cm^{-2} and it stays relatively constant after annealing at higher fluences such as 0.4 and 0.5 J cm^{-2}. This can be correlated to the formation of low resistivity NiSi after the 20-pulsed laser annealing at 0.3 J cm^{-2} and grain growth of NiSi phase after annealing at higher laser fluences.

One of the factors causing the reaction enhancement during multiple pulse laser annealing is laser induced surface roughening. From scanning electron microscopy (SEM) observations (not shown), the surface roughness was increased after the 20-pulsed laser annealing as compared to a single-pulsed laser annealing at 0.3 J cm^{-2}. TiO_x formed on the sample surface might affect the surface roughness. To measure the enhancement of the surface absorption due to laser induced surface roughening of the sample after laser annealing with different pulses at 0.3 J cm^{-2}, UV-visible analyses were performed. A monochromatic light with varying wavelength of 200–400 nm was used during the analysis, and the diffuse surface reflectance of the sample at 248 nm (the wavelength of the laser used during the laser annealing pro-

Downloaded 30 Jun 2011 to 155.69.4.4. Redistribution subject to AIP license or copyright; see http://jap.aip.org/about/rights_and_permissions

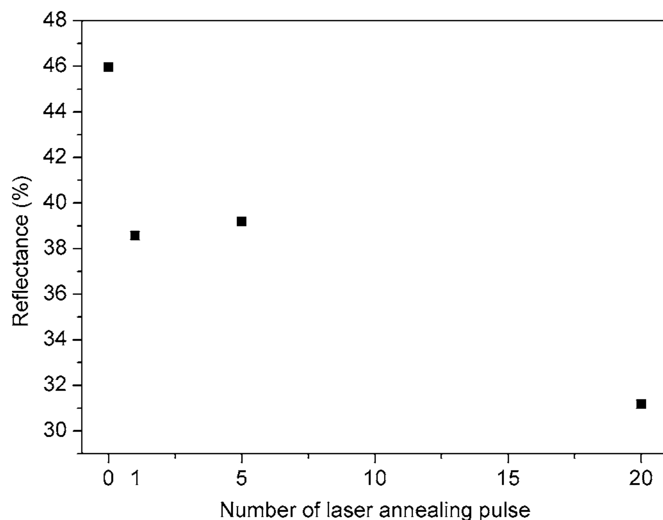

FIG. 6. The diffuse surface reflectance (obtained from UV-visible measurement at 248 nm laser wavelength) of the sample after 0.3 J cm^{-2} laser annealing at different laser pulses. The reflectance values were taken for the as-deposited sample and after 1-pulsed, 5-pulsed, and 20-pulsed laser annealings which were labeled as 0, 1, 5, and 20 in the x axis.

cess) was extracted and plotted in Fig. 6. A reduction of the diffuse surface reflectance (from 46% in the as-deposited sample down to about 31% after the 20-pulsed laser annealing at 0.3 J cm^{-2}) is obvious.

Other than poorer reflectance, the amorphous overlayer (as seen in Fig. 2) usually has a lower thermal conductivity, lower latent heat of melting, and lower T_m as compared to its crystalline counterparts.[24] These properties might cause the generation of a higher surface temperature in the sample during the subsequent multiple pulse laser annealing. On the other hand, the compound that was formed during the preceding laser irradiation might have lower T_m. For example, $NiSi_2$ phase, which formed after the five-pulsed laser annealing at 0.5 J cm^{-2} as observed in the XRD spectra shown in Fig. 1, melts at temperature as low as 993 °C.[18] This made the subsequent laser irradiation, coupled with an enhancement of surface absorbance and/or the presence of an amorphous layer, to cause a remelting of the existing low T_m compound, resulting in a deeper melting of the film. This prolonged the melt duration, allowing the elements in the film to mix evenly to form NiSi compound which was observed after the 20-pulsed laser annealing at 0.3 J cm^{-2}.

IV. CONCLUSION

Multiple-pulsed laser irradiation has been found to promote uniform elemental mixing during the reaction of $Ni_{1-x}(Ti)_x$ film on Si substrate and has led to the formation of NiSi phase. At the low fluence regime ($\leqslant$0.3 J cm^{-2}), the reaction occurred through a solid-state reaction similar to the conventional RTA annealing. Increasing the laser fluence has caused deeper melting and hence formation of silicon-rich silicide compound at the melt/Si interface. Enhancement in laser energy absorption that occurred during multiple-pulsed laser annealing was due to laser induced surface roughening and presence of amorphous overlayer. This increased the temperature generated in the sample for subsequent laser pulses which in turn improves the intermixing of the elements and resulted in the formation of NiSi. Furthermore, constitutional supercooling (CSC) phenomenon which usually results in a formation of cellular structure in laser annealed sample can also be alleviated. Our results demonstrate the possibility of achieving an optimum laser annealing condition in producing NiSi film using multiple-pulsed laser annealing.

ACKNOWLEDGMENTS

This work was financed in part by Special Projects, Chartered Semiconductor Manufacturing, and A*STAR Grant No. 0321010007.

[1] Z. Shi-Li and M. Östling, Crit. Rev. Solid State Mater. Sci. **28**, 1 (2003).
[2] S. P. Murarka, Intermetallics **3**, 173 (1995).
[3] P. S. Lee, D. Mangelinck, K. L. Pey, J. Ding, J. Y. Dai, C. S. Ho, and A. See, Microelectron. Eng. **51–52**, 583 (2000).
[4] W. L. Tan, K. L. Pey, S. Y. M. Chooi, J. H. Ye, and T. Osipowicz, J. Appl. Phys. **91**, 2901 (2002).
[5] W. L. Tan, K. L. Pey, S. Y. M. Chooi, and J. H. Ye, Mater. Res. Soc. Symp. Proc. **670**, K661 (2001).
[6] R. T. P. Lee, D. Z. Chi, M. Y. Lay, N. L. Yakovlev, and S. J. Chua, J. Electrochem. Soc. **151**, G642 (2004).
[7] R. T. Tung, J. M. Gibson, D. C. Jacobson, and J. M. Poate, Appl. Phys. Lett. **43**, 476 (1983).
[8] Y. F. Chong, K. L. Pey, A. T. S. Wee, A. See, L. Chan, Y. F. Lu, W. D. Song, and L. H. Chua, Appl. Phys. Lett. **76**, 3197 (2000).
[9] V. Privitera, C. Spinella, G. Fortunato, and L. Mariucci, Appl. Phys. Lett. **77**, 552 (2002).
[10] Y. Setiawan, P. S. Lee, K. L. Pey, X. C. Wang, and G. C. Lim, Appl. Phys. Lett. **88**, 113108 (2006).
[11] L. Lu and M. O. Lai, J. Appl. Phys. **94**, 4291 (2003).
[12] J.-S. Luo, W.-T. Lin, C. Y. Chang, and P. S. Shih, Nucl. Instrum. Methods Phys. Res. B **169**, 124 (2000).
[13] J.-S. Luo, W.-T. Lin, C. Y. Chang, P. S. Shih, and F. M. Pan, J. Vac. Sci. Technol. A **18**, 143 (2000).
[14] F. L. Chow, K. L. Pey, P. S. Lee, C. H. Tung, X. W. Wang, G. C. Lim, and Y. F. Chong, Electrochem. Solid-State Lett. **7**, G213 (2004).
[15] P. Baeri, M. G. Grimaldi, F. Priolo, A. G. Cullis, and N. G. Chew, J. Appl. Phys. **66**, 861 (1989).
[16] JCPDS-International Center for Diffraction Data, Card No. 44-1294 Ti, 2004 (unpublished).
[17] JCPDS-International Center for Diffraction Data, Card No. 04-0850 Ni, 2004 (unpublished).
[18] T. B. Massalski, *Binary Alloy Phase Diagrams* (American Society for Metals, Metals Park, OH, 1986).
[19] Y. Setiawan, P. S. Lee, C. W. Tan, and K. L. Pey, Thin Solid Films **504**, 153 (2006).
[20] R. T. Tung, J. M. Gibson, and J. M. Poate, Phys. Rev. Lett. **50**, 429 (1983).
[21] M. Hietschold, S. Schulze, U. Falke, F. Fenske, and W. Wolke, Appl. Surf. Sci. **102**, 156 (1996).
[22] M. von Allmen, S. S. Lau, T. T. Sheng, and M. Wittmer, in *Laser and Electron Beam Processing of Materials*, edited by C. W. White and P. S. Peercy (Academic, New York, 1980), p. 524.
[23] B. E. P. Beeston, R. W. Horne, and R. Markham, *Electron Diffraction and Optical Diffraction Techniques* (American Elsevier, New York, 1972).
[24] J. M. Poate and J. W. Mayer, *Laser Annealing of Semiconductors* (Academic, New York, 1982).

Downloaded 30 Jun 2011 to 155.69.4.4. Redistribution subject to AIP license or copyright; see http://jap.aip.org/about/rights_and_permissions